

Flavor in Ninths and a Discrete Gauge Origin of the QCD Axion

Vernon Barger¹

¹*Department of Physics, University of Wisconsin–Madison, Madison, Wisconsin 53706, USA*
(Dated: March 13, 2026)

Quark and lepton hierarchies are organized by rational powers of a single parameter in units of one ninth. We show that this “flavor in ninths” structure points to a discrete \mathbb{Z}_{18} gauge origin of Froggatt–Nielsen symmetry, whose \mathbb{Z}_9 subgroup controls the flavor lattice. Identifying the flavon with the Peccei–Quinn field, the same symmetry stabilizes the QCD axion, enforces domain-wall number $N_{\text{DW}} = 1$, and predicts the axion–photon coupling through the anomaly ratio $E/N = 8/3$ (or 2 with light higgsinos). The lowest Planck-suppressed operator appears at dimension eighteen, naturally solving the axion quality problem. For $f_a \sim (5\text{--}8) \times 10^{11}$ GeV the axion accounts for dark matter and lies within near-term haloscope reach.

I. INTRODUCTION

The Peccei–Quinn (PQ) mechanism dynamically solves the strong CP problem by promoting θ to an axion field whose vacuum expectation value relaxes $\bar{\theta} \rightarrow 0$ [1–3]; for reviews see Refs. [4, 5]. In any realistic theory, however, PQ must be an *extremely good* symmetry: Planck-suppressed PQ-violating operators can shift the axion minimum and reintroduce $\bar{\theta}$ [6–8]. A compelling cure is to realize PQ as an accidental symmetry emerging from a *discrete gauge* symmetry, which is expected to be respected by quantum gravity [9, 10] and is constrained by discrete anomaly conditions [11, 12].

Independently, fermion masses span many orders of magnitude yet exhibit structured hierarchies. In Froggatt–Nielsen (FN) theories [13], Yukawa couplings arise from higher-dimensional operators suppressed by a flavon vacuum expectation value (vev), schematically

$$y_{ij} \left(\frac{\Phi}{\Lambda} \right)^{p_{ij}} \bar{\psi}_i \psi_j H, \quad (1)$$

with exponents fixed by charges. Standard implementations of the FN mechanism assign integer charges and produce integer exponents [14, 15]. We observe, however, that quark and lepton hierarchies are accurately organized by *rational* exponents quantized in units of $1/9$, as established in a series of companion papers [16–19]. We argue that “flavor in ninths” is a low-energy imprint of a gauged \mathbb{Z}_{18} selection rule whose \mathbb{Z}_9 subgroup governs the flavor sector. Remarkably, if the FN flavon Φ is identified with the PQ field, the *same* \mathbb{Z}_{18} structure both generates the ninths flavor lattice and automatically solves the axion quality and domain-wall problems [20].

A related unification of the FN and PQ mechanisms via a continuous gauged $U(1)_F$ flavor symmetry has been developed independently in Ref. [21]. A key distinction is that our discrete \mathbb{Z}_{18} fixes the leading PQ-violating operator dimension *exactly* (dimension 18), whereas in continuous $U(1)_F$ constructions the quality argument depends on the pattern of symmetry breaking and the resulting residual discrete subgroup. Integer-charge FN models have also been studied systematically by Cornella, Curtin, Neil, and Thompson [22, 23]. Those con-

structions map all solutions to the quark flavor problem within the standard integer-charge FN framework, providing a useful benchmark: the ninths lattice is excluded by construction in that search because it requires rational charges with denominator nine. We comment further on this comparison in Sec. VIII.

The rest of this paper is organized as follows. Section II establishes the phenomenological basis for the ninths lattice, derives the expansion parameter $B = 75/14$, and presents quark and lepton exponent matrices. Section III connects the ninths quantization to a gauged \mathbb{Z}_{18} symmetry and presents a complete set of charge assignments satisfying discrete anomaly cancellation. Section IV shows that identifying the flavon with the PQ field yields automatic axion quality and $N_{\text{DW}} = 1$. Section V works out the axion phenomenology, including E/N , the axion–photon and axion–electron couplings, and the cosmological relic density. Section VI discusses the extension to the neutrino sector and the Pontecorvo–Maki–Nakagawa–Sakata (PMNS) matrix. Section VII describes the vector-like messenger sector that provides the UV completion of the rational exponents. Section VIII compares the ninths framework with integer-charge FN models. Section IX summarizes the unified picture. Five appendices collect the anomaly verification, the E/N calculation, details of the messenger chain construction, a terminology guide, and worked examples of mass ratios and CKM elements in the hop framework.

II. NINTHS STRUCTURE AND TEXTURES

A. Determination of the expansion parameter

The central claim is that a single expansion parameter $\epsilon \equiv \langle \Phi \rangle / \Lambda = 1/B$ controls all quark and lepton hierarchies. The value of B is determined by the two best-measured Cabibbo–Kobayashi–Maskawa (CKM) [24, 25] magnitudes together with their ninths exponents:

$$|V_{us}| = \epsilon^{8/9}, \quad |V_{cb}| = \epsilon^{17/9}. \quad (2)$$

TABLE I. Ninths scalings versus data. Predicted values use $\epsilon = 14/75 \approx 0.187$. Quark mass ratios are evaluated at $\mu \sim 10^2$ GeV using the running masses of Ref. [28].

Observable	Exponent	ϵ^p	Data
$ V_{us} $	8/9	0.225	0.225
$ V_{cb} $	17/9	0.042	0.042
$ V_{ub} $	10/3	0.0037	0.0038
m_s/m_b	7/3	0.020	0.019
m_c/m_t	10/3	0.0037	0.0036
m_μ/m_τ	5/3	0.061	0.060
m_e/m_μ	29/9	0.0045	0.0048

Taking the Particle Data Group (PDG) central values $|V_{us}| = 0.2250$ and $|V_{cb}| = 0.04182$ [26], Eq. (2) gives

$$B = |V_{us}|^{-9/8} = 5.357, \quad B = |V_{cb}|^{-9/17} = 5.358, \quad (3)$$

in remarkable agreement. The ratio $75/14 \simeq 5.357$ provides a convenient exact rational representation; the corresponding expansion parameter is $\epsilon = 14/75 \approx 0.1867$.

The system is overdetermined: once B is fixed by $|V_{us}|$ and $|V_{cb}|$, the remaining CKM element $|V_{ub}|$ and the quark and lepton mass ratios become predictions. Their numerical quality is summarized in Table I.

B. CKM scalings

With $\epsilon \approx 0.187$, the three independent CKM magnitudes are well described by

$$|V_{us}| \sim \epsilon^{8/9}, \quad |V_{cb}| \sim \epsilon^{17/9}, \quad |V_{ub}| \sim \epsilon^{10/3}. \quad (4)$$

In the FN language of Eq. (1), such relations reflect additive charge relations among generations and are naturally reproduced when the charge differences themselves are quantized in ninths. The Jarlskog invariant [27] scales as $J \sim \epsilon^{8/9+17/9+10/3} \sin \delta = \epsilon^{55/9} \sin \delta$, giving $J \approx 3.5 \times 10^{-5} \sin \delta$, consistent with the measured value $J = (3.08 \pm 0.13) \times 10^{-5}$ [26] for $\sin \delta \approx 0.88$.

C. Mass ratio scalings

Quark mass ratios align with the same expansion parameter:

$$\frac{m_s}{m_b} \sim \epsilon^{7/3}, \quad \frac{m_c}{m_t} \sim \epsilon^{10/3}, \quad (5)$$

suggesting that *both* mixings and masses are controlled by exponents in $\frac{1}{9}\mathbb{Z}$ rather than integers. The first-generation quark mass ratios m_d/m_s and m_u/m_c involve the lightest quarks, whose running masses carry larger uncertainties and whose textures are most sensitive to $\mathcal{O}(1)$ coefficients. In the companion papers [17, 18], the down-quark mass ratio $m_d/m_s \sim \epsilon^{10/9}$ is reproduced

with an $\mathcal{O}(1)$ coefficient c_d of order unity, while the extreme smallness of m_u requires either $m_u/m_c \sim \epsilon^{34/9}$ (purely from the texture) or a partial cancellation among $\mathcal{O}(1)$ prefactors. The ninths lattice determines the parametric scaling but does not fully fix these first-generation ratios; we defer their detailed treatment to Refs. [17, 18].

D. Quark exponent matrices

A representative set of exponent matrices illustrating the ninths quantization is

$$p_{ij}^u = \frac{1}{9} \begin{pmatrix} 64 & 39 & 27 \\ 55 & 30 & 18 \\ 37 & 12 & 0 \end{pmatrix}, \quad (6)$$

$$p_{ij}^d = \frac{1}{9} \begin{pmatrix} 37 & 30 & 27 \\ 28 & 21 & 18 \\ 10 & 3 & 0 \end{pmatrix}.$$

These follow from the additive rule $p_{ij} = Q(q_i) + Q(q_j^c)$ with the charge assignments in Table II: left-handed charges $Q(Q_i) = (3, 2, 0)$, right-handed up-type charges $Q(u_j^c) = (37/9, 4/3, 0)$, and right-handed down-type charges $Q(d_j^c) = (10/9, 1/3, 0)$. The unsuppressed $(3, 3)$ entries follow from $Q(Q_3) = Q(u_3^c) = Q(d_3^c) = 0$; the stepwise suppressions in ninths capture the observed hierarchies and are stable under diagonalization (not a basis artifact). Concrete charge assignments and full texture fits are presented in the companion papers [17, 18]. Worked examples showing how specific mass ratios and CKM elements emerge from the hop framework are collected in Appendix E.

E. Lepton exponent matrices

Beyond quarks, the charged-lepton mass ratios are reproduced by the same expansion parameter with ninths exponents,

$$\frac{m_\mu}{m_\tau} \sim \epsilon^{5/3}, \quad \frac{m_e}{m_\mu} \sim \epsilon^{29/9}, \quad (7)$$

as shown in Table I. The charged-lepton exponent matrix, using left-handed doublet charges $Q(L_i) = (1, 1/2, 0)$ and right-handed charges $Q(e_j^c) = (23/6, 7/6, 0)$ from Table II, takes the form

$$p_{ij}^\ell = \frac{1}{6} \begin{pmatrix} 29 & 13 & 6 \\ 26 & 10 & 3 \\ 23 & 7 & 0 \end{pmatrix}. \quad (8)$$

For neutrinos, the effective Majorana mass matrix arises from the dimension-five Weinberg operator [29]

$LLHH/\Lambda_\nu$ and is symmetric in the lepton-doublet indices, giving exponents $p_{ij}^\nu = Q(L_i) + Q(L_j)$:

$$p_{ij}^\nu = \begin{pmatrix} 2 & 3/2 & 1 \\ 3/2 & 1 & 1/2 \\ 1 & 1/2 & 0 \end{pmatrix}. \quad (9)$$

The mass eigenvalue hierarchy is $m_1 : m_2 : m_3 \sim \epsilon^2 : \epsilon : 1$, corresponding to normal ordering. Large atmospheric mixing ($\theta_{23} \sim 45^\circ$) requires the $\mathcal{O}(1)$ coefficients in the 23 block to exhibit approximate μ - τ symmetry; this is a condition on the coefficients, not on the exponents. We note that the texture in Eq. (9) follows from strict charge additivity and therefore has a hierarchical 23 block (entries 1, 1/2, 1/2, 0). In the companion lepton-lattice paper [19], the effective neutrino texture instead adopts a flat 23 block with $p_{22}^\nu = p_{23}^\nu = p_{33}^\nu = 0$, enforced by a messenger selection rule that freezes the second- and third-generation lepton-doublet charges at the same effective value. The flat structure embeds μ - τ symmetry directly in the exponents rather than relying on $\mathcal{O}(1)$ coefficients alone, and is responsible for the sharp octant- δ_{CP} correlation found there. Both textures reproduce the same mass eigenvalue hierarchy; they differ in the mechanism for large θ_{23} , and the choice between them is ultimately a question about the messenger sector in the lepton doublet channel. We return to the neutrino sector in Sec. VI.

The unification of quark and lepton textures in a single ninths lattice is one of the main phenomenological motivations for seeking a discrete gauge origin. From the model-building perspective, the ninths quantization is unusually robust: adding heavy messenger chains shifts exponents by integers, but cannot spoil the underlying 1/9 granularity. This makes the ninths lattice a clean discriminator between genuinely discrete-charge constructions and purely continuous FN models with arbitrary rational charges. In practice, the lattice pins down which texture deformations are allowed at a given order in ϵ , and this is what enables sharp statements about CKM angles and CP phases in the companion analyses [17, 18].

III. \mathbb{Z}_{18} ORIGIN, NINTHS SUBSTRUCTURE, AND ANOMALY CONSISTENCY

A. Ninths from \mathbb{Z}_9

The ninths lattice suggests that FN charges are defined modulo nine. A minimal way to generate all residues is a set of flavon charges $(1, 2, 4) \pmod{9}$, Fig. 1. Equivalently, all effective FN charges may be written as

$$q_i = \frac{k_i}{9}, \quad k_i \in \mathbb{Z}, \quad (10)$$

and operator selection is the statement that total charge is an integer.

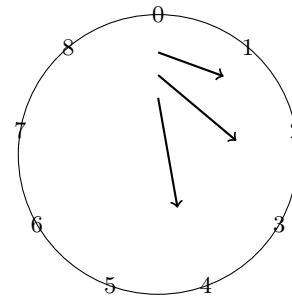


FIG. 1. \mathbb{Z}_9 flavor subgroup of \mathbb{Z}_{18} . The generators $(1, 2, 4)$ span all residues mod 9, enabling suppressions quantized in $1/9$.

Yukawa operators obey discrete invariance conditions, e.g.

$$X(Q_i) + X(u_j) + X(H_u) \equiv 0 \pmod{9}, \quad (11)$$

and similarly for down-type and lepton operators, enforcing that every FN suppression exponent lies in $\frac{1}{9}\mathbb{Z}$. In this sense, the continuous FN symmetry is an accidental low-energy remnant of a gauged \mathbb{Z}_{18} selection rule, with the flavor sector controlled by its \mathbb{Z}_9 subgroup.

The point of the $(1, 2, 4)$ choice is that it is *minimal* in a strong sense: these charges, being $\{2^0, 2^1, 2^2\}$, correspond to $N_{\text{hop}} = 3$ distinct types of nearest-neighbor hop on a chain of $N_{\text{site}} = 4$ vectorlike messenger sites. (The chain sites carry \mathbb{Z}_9 charges $(0, 8, 6, 2)$; the hop charges $(1, 2, 4)$ are the differences between adjacent sites, since $0 - 8 \equiv 1$, $8 - 6 = 2$, $6 - 2 = 4 \pmod{9}$. Thus $N_{\text{hop}} = N_{\text{site}} - 1$.) Every residue mod 9 can be reached as a non-negative integer combination of the three hop charges with total hop count $n_{\text{tot}} \equiv n_1 + n_2 + n_3$ at most three, so that no FN exponent requires more than three flavon insertions. (Here n_a denotes the number of hops of type a , each hop contributing charge $q_a/9$; n_{tot} is the total number of hops, which should not be confused with the fixed number of hop types $N_{\text{hop}} = 3$ or the number of chain sites $N_{\text{site}} = 4$.) No two-element subset of hop charges achieves this—e.g. the pair $(1, 2)$ requires n_{tot} up to four. As a result, the allowed singlet monomials built from flavons with these charges satisfy the congruence

$$n_1 + 2n_2 + 4n_3 \equiv 0 \pmod{9}, \quad (12)$$

which directly controls the spectrum of FN suppressions. The full \mathbb{Z}_{18} imposes a stronger constraint on PQ-violating scalar operators: since the flavon carries the minimal \mathbb{Z}_{18} charge, the first gauge-invariant pure-flavon monomial is Φ^{18} , not Φ^9 .

B. Charge assignments

The Froggatt–Nielsen charges that reproduce the textures in Eqs. (6)–(9) via the additive rule $p_{ij} = Q(\psi_i) +$

TABLE II. Froggatt–Nielsen charge assignments. The three quark-doublet generations are Q_i , $i = 1, 2, 3$; similarly for right-handed up quarks u_i^c , down quarks d_i^c , lepton doublets L_i , and right-handed charged leptons e_i^c . The Yukawa exponent is $p_{ij} = Q(\psi_i) + Q(\psi_j^c)$. Charges are taken from Refs. [17, 19].

Field	Gen. 1	Gen. 2	Gen. 3
Q_i	3	2	0
u_i^c	37/9	4/3	0
d_i^c	10/9	1/3	0
L_i	1	1/2	0
e_i^c	23/6	7/6	0

$Q(\psi_j^c)$ are given in Table II. These are the charges established in the companion two-over-two paper [17]; the lepton charges include the corrections from the companion lepton-lattice paper [19]. All charges lie on the 1/18 sublattice (i.e. $18Q$ is an integer for every field), consistent with the \mathbb{Z}_{18} discrete gauge symmetry. The embedding of these FN charges into a self-consistent set of \mathbb{Z}_{18} integer charges, including the chain messenger sector, is developed in detail in the companion unified flavor paper [30].

One can verify from Table II that, for example, the down-type (1,1) exponent is

$$p_{11}^d = Q(Q_1) + Q(d_1^c) = 3 + \frac{10}{9} = \frac{37}{9}, \quad (13)$$

matching the (1,1) entry of p_{ij}^d in Eq. (6). The unsuppressed (3,3) entries follow from $Q(Q_3) = Q(u_3^c) = Q(d_3^c) = 0$. The exponent *differences* (which control mass ratios and mixing angles) are the physically meaningful quantities, and the charge assignments in Table II reproduce all seven entries of Table I with $\mathcal{O}(1)$ coefficients close to unity [17].

C. Anomaly cancellation

If \mathbb{Z}_{18} is a discrete gauge symmetry, it is constrained by mixed anomaly conditions. A compact statement is

$$A_G \equiv \sum_i X_i \ell(r_i) = 0 \pmod{18}, \quad (14)$$

for each gauge factor G , where X_i is the \mathbb{Z}_{18} charge and $\ell(r_i)$ the Dynkin index of the representation of the i th chiral fermion, following the standard discrete anomaly conditions of Refs. [11, 12]. For the SM gauge group $SU(3)_C \times SU(2)_L \times U(1)_Y$, the three anomaly sums $A_{SU(3)}$, $A_{SU(2)}$, and the mixed \mathbb{Z}_{18} –gravity anomaly must each vanish mod 18. The explicit verification—including the contributions from the $N_{\text{site}} = 4$ vectorlike messenger pairs described in Sec. VII—is given in the companion papers [17, 30]; a summary is provided in Appendix A.

In a minimal UV completion, the chain has $N_{\text{site}} = 4$ sites carrying \mathbb{Z}_9 charges (0, 8, 6, 2), connected by $N_{\text{hop}} = 3$ links with hop charges (1, 2, 4). All four sites are new heavy vectorlike messenger pairs $D_a + \bar{D}_a$ ($a = 1, 2, 3, 4$) with masses $M_a \sim \Lambda$; the SM right-handed quarks $d_{R,j}$ couple to D_1 and the SM left-handed doublets $q_{L,i}$ couple to D_4 via endpoint Yukawa operators [30]. Integrating out all four VLQ pairs at tree level generates the FN operators in Eq. (1), with the number of hops n_a of each type determining the suppression exponent. These messengers also enter the anomaly sums in Eq. (14), and their \mathbb{Z}_{18} charges must be chosen to satisfy the anomaly-cancellation conditions jointly with the SM fermions.

IV. AXION QUALITY FROM NINTHS AND $N_{\text{DW}} = 1$

We now identify the FN flavon with the PQ field, so that Φ carries the minimal \mathbb{Z}_{18} charge $q_\Phi = 1/18$. Any gauge-invariant singlet monomial must satisfy $nq_\Phi \in \mathbb{Z}$, hence $n = 18$ is the first allowed power. Therefore the leading Planck-suppressed PQ-violating operator is

$$\Delta\mathcal{L} \supset \frac{c_{18}}{M_{\text{Pl}}^{14}} \Phi^{18} + \text{h.c.}, \quad (15)$$

with $c_{18} = \mathcal{O}(1)$. This induces a shift in the axion minimum scaling as

$$\Delta\bar{\theta} \sim \left(\frac{f_a}{M_{\text{Pl}}}\right)^{14} \left(\frac{f_a}{\Lambda_{\text{QCD}}}\right)^4, \quad (16)$$

where the second factor arises from the ratio of the PQ-breaking potential to the QCD topological susceptibility $\chi_{\text{top}} \sim \Lambda_{\text{QCD}}^4$. For $f_a \sim 10^{12}$ GeV, $(f_a/M_{\text{Pl}})^{14} \sim 10^{-90}$ overwhelms the enhancement $(f_a/\Lambda_{\text{QCD}})^4 \sim 10^{51}$, giving $\Delta\bar{\theta} \lesssim 10^{-39} \ll 10^{-10}$. Thus axion quality is automatic in the ninths framework.

This should be contrasted with generic DFSZ (Dine–Fischler–Srednicki–Zhitnitsky) and KSVZ (Kim–Shifman–Vainshtein–Zakharov) constructions [31–33], where the leading PQ-breaking operator is typically allowed already at relatively low dimension ($n \leq 10$) unless additional ad hoc symmetries are imposed [6–8, 10, 34, 35]. For instance, in a model with only a \mathbb{Z}_N symmetry protecting PQ, the operator Φ^N appears at dimension N ; maintaining $\Delta\bar{\theta} < 10^{-10}$ requires $N \geq 12$ for $f_a \sim 10^{12}$ GeV [6–8]. In the present framework, the prohibition of all operators Φ^n with $n < 18$ is a direct consequence of the same \mathbb{Z}_{18} arithmetic whose \mathbb{Z}_9 subgroup enforces the ninths flavor lattice, so axion quality is not an extra assumption but a corollary of the flavor structure, with a generous margin of safety.

Since the flavon is the PQ field, the flavor expansion parameter is directly $\epsilon = f_a/\Lambda$, linking the messenger scale to the axion decay constant: $\Lambda = f_a/\epsilon \sim (3\text{--}4) \times 10^{12}$ GeV for $f_a \sim (5\text{--}8) \times 10^{11}$ GeV. The flavor hierarchy

and the axion mass window thus trace back to a single dimensionless ratio.

The same discrete origin fixes the domain-wall number. The QCD anomaly coefficient is

$$N = \sum_{\text{colored Weyl } i} X_i. \quad (17)$$

Using Yukawa invariance (e.g. Eq. (11) and its down-type analogue), one finds that generation-dependent contributions cancel identically in the anomaly, leaving a single overall PQ rotation. More explicitly, summing over three generations of (Q_i, u_i^c, d_i^c) :

$$\begin{aligned} N &= \sum_{i=1}^3 [X(Q_i) + X(u_i^c) + X(d_i^c)] \\ &= -3[X(H_u) + X(H_d)], \end{aligned} \quad (18)$$

where the second line follows from the Yukawa invariance conditions: $X(u_i^c) = -X(Q_i) - X(H_u)$ and $X(d_i^c) = -X(Q_i) - X(H_d)$, so each generation contributes $-X(H_u) - X(H_d)$ independent of i . This is a standard result for DFSZ-type models [5]. In the minimal realization where the two Higgs doublets carry equal and opposite PQ charges relative to the flavon normalization, the integer domain-wall number is

$$N_{\text{DW}} = 1. \quad (19)$$

The detailed \mathbb{Z}_{18} charge assignments and the verification that $N_{\text{DW}} = 1$ in the full model (including the chain messenger sector) are given in the companion papers [17, 30]. Hence the string-wall system annihilates without a stable wall network, avoiding the domain-wall catastrophe identified by Sikivie [20].

V. E/N AND AXION PHENOMENOLOGY

A. E/N derivation

The electromagnetic anomaly is

$$E = \sum_i X_i Q_i^2, \quad (20)$$

where Q_i is the electric charge of the i th fermion, and the axion-photon coupling is

$$g_{a\gamma\gamma} = \frac{\alpha}{2\pi f_a} \left(\frac{E}{N} - 1.92 \right), \quad (21)$$

with α the fine-structure constant and 1.92 the model-independent QCD contribution.

Using Yukawa invariance, the anomaly sums in Eqs. (17) and (20) can be reorganized so that E and N depend only on a small set of Higgs and matter-charge combinations. The key step is that for each generation the Yukawa conditions $X(Q_i) + X(u_i^c) + X(H_u) \equiv 0$

and $X(Q_i) + X(d_i^c) + X(H_d) \equiv 0$ allow elimination of right-handed charges in favor of left-handed and Higgs charges. Summing over all colored and electromagnetically charged fermions, the generation-dependent pieces cancel (as in the N computation above), leaving

$$E = N_g \left[\frac{2}{3} X(H_u) + \frac{1}{3} X(H_d) \right] + E_\ell, \quad (22)$$

where $N_g = 3$ is the number of generations and E_ℓ is the lepton contribution, which similarly reduces to Higgs charges via the lepton Yukawa invariance. For the minimal non-supersymmetric two-Higgs-doublet realization (DFSZ-II), the explicit evaluation (detailed in Appendix B) yields

$$\frac{E}{N} = \frac{8}{3}, \quad (23)$$

the canonical DFSZ-II value. In supersymmetric completions, the higgsinos contribute additional colored and charged states to the anomaly sums [36]; with light higgsinos ($\mu \lesssim f_a$), this shifts the ratio to

$$\frac{E}{N} = 2, \quad (24)$$

recovering $8/3$ when higgsinos are decoupled ($\mu \gg f_a$). The full derivation is given in Appendix B.

It is useful to contrast these predictions with the KSVZ benchmark. In KSVZ models [31, 32], the axion couples to photons only through heavy colored fermions and the model-independent QCD contribution, giving $E/N = 0$; the resulting coupling $|g_{a\gamma\gamma}^{\text{KSVZ}}| = \alpha \cdot 1.92 / (2\pi f_a)$ is about a factor of 2.3 larger than the DFSZ-II value at the same f_a , since $|8/3 - 1.92| \simeq 0.75$ while $|0 - 1.92| = 1.92$. This is why current ADMX runs have already reached KSVZ-level sensitivity over portions of the μeV range, while the DFSZ-II band remains a near-term target. The ninths framework thus makes a sharp prediction: the axion-photon coupling should lie on the weaker DFSZ-II line in the non-supersymmetric case, or be further suppressed ($|E/N - 1.92| \simeq 0.08$) in the supersymmetric case with $E/N = 2$, well below the KSVZ line.

B. Axion mass and couplings

The axion mass is

$$m_a \simeq 5.7 \mu\text{eV} \left(\frac{10^{12} \text{ GeV}}{f_a} \right), \quad (25)$$

so $f_a \sim (5-8) \times 10^{11} \text{ GeV}$ corresponds to $m_a \sim 7-12 \mu\text{eV}$. For these values, Eq. (21) implies $g_{a\gamma\gamma} \sim (1-2) \times 10^{-15} \text{ GeV}^{-1}$, within projected haloscope sensitivity.

Haloscope searches probe this parameter space by resonant conversion of halo axions to photons in a tunable cavity; the target masses correspond to microwave frequencies $\nu \simeq m_a / (2\pi) \sim (1.7-3) \text{ GHz}$. Recent ADMX runs have reached KSVZ-level sensitivity over portions of

the μeV range [37], and continued improvements aim to close the remaining factor of ~ 2.3 in coupling strength needed to reach the DFSZ-II band; a convenient summary of current limits and projections is given in the PDG review [38] and in the comprehensive survey of Ref. [5]. The predicted mass window is therefore experimentally actionable: it is narrow enough to motivate focused scanning strategies, yet broad enough to accommodate the current simulation systematics in the post-inflationary abundance. In addition, the two discrete predictions $N_{\text{DW}} = 1$ and E/N correlate cosmology with laboratory reach: the same charge assignment that guarantees network collapse also fixes the conversion strength relevant for haloscopes.

As a DFSZ-II-type model, the axion also couples to electrons at tree level with $g_{aee} \sim m_e \cos^2\beta/(3f_a) \sim \mathcal{O}(10^{-16})$ for $f_a \sim 10^{12}$ GeV, where $\tan\beta$ is the ratio of Higgs vacuum expectation values. This is consistent with present astrophysical bounds from white-dwarf cooling and red-giant luminosity functions [38], and lies within the projected sensitivity of next-generation direct-detection experiments.

C. Cosmological relic density

In the post-inflationary scenario (PQ broken after inflation), the axion relic density receives contributions from misalignment and from radiation by the string-wall network (see Ref. [39] for a comprehensive review of axion cosmology). Recent large-scale simulations find a mild power-law dependence on f_a ; a convenient summary is

$$\Omega_a h^2 \simeq 0.12 \left(\frac{f_a}{(5-7) \times 10^{11} \text{ GeV}} \right)^{1.165}, \quad (26)$$

with $\mathcal{O}(1)$ systematic uncertainty from the network dynamics [40–42]. With $N_{\text{DW}} = 1$, the network collapses, and Eq. (26) naturally reproduces the observed dark matter density in the μeV mass window. The argument is structural: $N_{\text{DW}} = 1$ is guaranteed by the same \mathbb{Z}_{18} charge assignments that enforce the ninths flavor lattice (Sec. IV), so the absence of a stable domain-wall network is not a model-building choice but a consequence of the flavor symmetry.

If PQ breaks before inflation, the relic density depends on the initial misalignment angle and is therefore less predictive; in addition, the CMB isocurvature bound independently requires $H_I \lesssim 10^7$ GeV ($f_a/10^{12}$ GeV), constraining the inflationary scale [43]. Nonetheless, the axion-quality argument and the anomaly predictions (N_{DW} and E/N) remain intact. In either cosmological history, the distinctive point is that the *same* discrete gauge structure simultaneously controls the flavor exponents and the dangerous PQ-breaking operators.

Equation (26) is intended as a compact phenomenological target rather than a precision prediction: the dominant uncertainty is the efficiency of axion emission from

the scaling string network and the subsequent wall collapse, which depends on the approach to scaling and on the radiated spectrum. Progress on these systematics continues [44], but the key point for the present work is structural: with $N_{\text{DW}} = 1$ the network necessarily annihilates, and the favored dark-matter window aligns naturally with the μeV mass range implied by $f_a \sim 10^{12}$ GeV.

VI. NEUTRINO SECTOR AND PMNS STRUCTURE

The neutrino exponent matrix in Eq. (9) gives mass eigenvalue scalings $m_1 : m_2 : m_3 \sim \epsilon^2 : \epsilon : 1$, corresponding to normal ordering with

$$\frac{m_2}{m_3} \sim \epsilon \approx 0.19, \quad \frac{m_1}{m_2} \sim \epsilon \approx 0.19. \quad (27)$$

Taking $m_3 \approx 50$ meV (from $\sqrt{\Delta m_{\text{atm}}^2}$), these predict $m_2 \approx 9$ meV and $m_1 \approx 1.7$ meV, consistent with the NuFIT 6.0 global fit [45].

The PMNS [46, 47] mixing matrix receives contributions from both the charged-lepton and neutrino diagonalization rotations: $U_{\text{PMNS}} = U_\ell^\dagger U_\nu$. In the ninths framework, the dominant features of the PMNS matrix are controlled by two distinct sources.

First, the atmospheric angle θ_{23} is largely determined by the $\mathcal{O}(1)$ coefficients in the neutrino 23 block. Approximate μ - τ symmetry [48, 49] among these coefficients naturally gives $\theta_{23} \sim 45^\circ$, consistent with near-maximal atmospheric mixing.

Second, the reactor angle θ_{13} and the solar angle θ_{12} receive contributions from the charged-lepton rotation U_ℓ , whose off-diagonal entries scale as $\epsilon^{1/2} \sim 0.43$ and $\epsilon \sim 0.19$. The resulting predictions are $\theta_{13} \sim \mathcal{O}(\epsilon^{1/2}) \sim 8$ – 9° and corrections to θ_{12} of order $\epsilon^{1/2}$, both compatible with data [45].

The CP-violating Dirac phase δ_{CP} in the PMNS matrix is predicted to lie in the range 250° – 310° , depending on the octant of θ_{23} ; the companion lepton-lattice paper [19] finds a correlation between the θ_{23} octant and δ_{CP} that will be tested by the Deep Underground Neutrino Experiment (DUNE) [50] and Hyper-Kamiokande [51]. The scheme favors normal mass ordering, which is also preferred by current global fits.

The effective Majorana mass for neutrinoless double-beta decay is predicted to be $m_{\beta\beta} \sim \epsilon^2 m_3 \sim 2$ meV in normal ordering, below current experimental sensitivity but within reach of next-generation ton-scale experiments.

VII. VECTORLIKE MESSENGER SECTOR

The rational FN exponents of the ninths lattice arise from a concrete UV mechanism: heavy vectorlike fermion chains connecting SM fields to the flavon, as illustrated in Fig. 2. In the minimal realization [17, 30], the chain

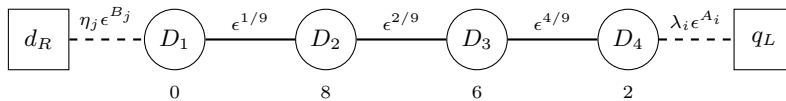


FIG. 2. Chain topology for the down-type messenger sector. Circles denote the $N_{\text{site}} = 4$ vectorlike quark pairs D_a ($a = 1, \dots, 4$) with \mathbb{Z}_9 site charges shown below. Solid lines are nearest-neighbor flavon couplings carrying the indicated hop suppression; dashed lines are endpoint Yukawa couplings [Eq. (C2)] to the SM quarks. The three hop charges (1, 2, 4) sum to 7/9, giving the internal chain suppression $\epsilon^{7/9} \simeq 0.27$. The total Yukawa suppression for entry (i, j) is the product of three factors: the entrance (left-handed endpoint) $\epsilon^{A_i/9}$, the internal chain $\epsilon^{7/9}$, and the exit (right-handed endpoint) $\epsilon^{B_j/9}$, giving $Y_{ij} \sim \epsilon^{(A_i+7+B_j)/9}$. Since the internal factor is common to all entries, mass ratios depend only on the endpoint dressings.

consists of $N_{\text{site}} = 4$ new vectorlike messenger pairs $D_a + \bar{D}_a$ ($a = 1, 2, 3, 4$) carrying \mathbb{Z}_9 charges (0, 8, 6, 2), connected by $N_{\text{hop}} = N_{\text{site}} - 1 = 3$ types of nearest-neighbor link with hop charges $(q_1, q_2, q_3) = (1, 2, 4)$. All four D_a are new heavy fields transforming as fundamentals under $SU(3)_C$; the SM quarks couple externally to the chain endpoints via $\bar{q}_{L,i} \tilde{H} D_4 (\Phi/\Lambda)^{A_i}$ and $\bar{D}_1 d_{R,j} (\Phi/\Lambda)^{B_j}$, where A_i and B_j are determined by the SM field charges [30]. The VLQ mass terms $M_a \bar{D}_a D_a$ with $M_a \sim \Lambda$ and nearest-neighbor couplings $\lambda_a \Phi \bar{D}_a D_{a+1}$ generate, upon integrating out the heavy states at tree level, effective Yukawa operators of the form

$$y_{\text{eff}} \sim \prod_{a=1}^{N_{\text{hop}}} \left(\frac{\lambda_a \langle \Phi \rangle}{M_a} \right)^{n_a}, \quad (28)$$

where n_a is the number of hops of type a and the FN exponent is $p_{ij} = \sum_a n_a \cdot (q_a/9)$. It is important to distinguish the number of chain sites $N_{\text{site}} = 4$ (which sets the messenger content), the number of hop types $N_{\text{hop}} = 3$ (which sets the charge granularity), and the hop multiplicities n_a (which vary from operator to operator); this terminology is summarized in Appendix D. The total hop count $n_{\text{tot}} = \sum_a n_a$ can range from zero (the unsuppressed (3, 3) entries) up to several for the most suppressed first-generation entries. The rational denominators arise because the \mathbb{Z}_9 charge of each hop is $q_a/9$, not an integer.

The key features of this construction are as follows.

Exponent quantization: every FN exponent is $p_{ij} = \sum_a n_a q_a/9$, a sum of n_a multiples of 1/9, 2/9, and 4/9, hence lies in $\frac{1}{9}\mathbb{Z}$ automatically.

Flavor-changing neutral current (FCNC) suppression: the messengers couple to SM quarks only at the chain endpoints, so FCNC amplitudes inherit the same ϵ -suppression as the Yukawa textures—a built-in Glashow–Iliopoulos–Maiani (GIM)-like mechanism [30].

No Landau poles: with four new vectorlike quark pairs ($N_{\text{site}} = 4$) at mass $M \sim \Lambda \sim \text{few} \times 10^{12}$ GeV, the one-loop beta function coefficient for $SU(3)_C$ shifts by $\Delta b_3 = +8/3$. The QCD coupling remains perturbative up to the Planck scale.

Collider signatures: if the lightest messenger has mass $M_D \sim \text{few TeV}$ (as suggested by naturalness of the flavor scale), it would be pair-produced at the Large Hadron Collider (LHC) via QCD processes, decaying as

$D \rightarrow bZ, bH, tW$ with branching ratios approximately 1 : 1 : 2 [52]. Current LHC searches constrain $M_D \gtrsim 1.5$ TeV [26]; the High-Luminosity LHC (HL-LHC) will extend this reach to ~ 2 TeV.

The chain construction and its perturbative diagonalization are developed in full detail in the companion unified flavor paper [30]. Appendix C provides a self-contained summary of the chain topology and the resulting exponent algebra.

VIII. COMPARISON WITH INTEGER-CHARGE FN MODELS

It is instructive to compare the ninths framework with the systematic integer-charge FN analyses of Cornella, Curtin, Neil, and Thompson [22, 23]. Those works enumerate all charge assignments with integer FN exponents that can reproduce the quark mass and mixing hierarchy within specified tolerance bands. Their approach provides a valuable landscape of solutions within the standard FN paradigm.

The ninths lattice lies outside this landscape by construction, since the defining feature is rational exponents with denominator nine. The key phenomenological distinctions are as follows.

Expansion parameter: integer-charge models typically use $\epsilon_C \sim |V_{us}| \approx 0.22$ (the Cabibbo parameter) or $\epsilon_C^{1/2}$, fitting CKM elements to integer powers thereof. The ninths framework uses $\epsilon = 0.187$, which is distinct from any simple root of $|V_{us}|$ and is instead fixed by the rational exponents 8/9 and 17/9 simultaneously.

Axion quality: in an integer-charge \mathbb{Z}_N model, the leading PQ-violating operator appears at dimension N . To achieve $\Delta\bar{\theta} < 10^{-10}$ with $f_a \sim 10^{12}$ GeV requires $N \geq 12$ [6–8]. The ninths framework automatically gives $N = 18$ as a consequence of the flavor structure, providing six extra units of safety margin.

Precision: Table I shows that the ninths exponents reproduce seven independent observables at the 1–6% level. Integer-exponent fits typically require $\mathcal{O}(1)$ coefficients of order 2–3 to absorb the mismatch between ϵ_C^n and the data; the rational exponents absorb this mismatch into the exponent itself, reducing the role of unknown coefficients.

TABLE III. Summary of discrete predictions from the \mathbb{Z}_{18} ninths framework.

Quantity	Prediction
$B = 1/\epsilon$	$75/14 \simeq 5.36$
ϵ	$14/75 \simeq 0.187$
N_{DW}	1
E/N (non-SUSY)	$8/3$
E/N (SUSY, light higgsinos)	2
Leading PQ-violating dim.	18
Λ (messenger scale)	$(3-4) \times 10^{12}$ GeV
m_a	$7-12$ μeV
$g_{a\gamma\gamma}$	$(1-2) \times 10^{-15}$ GeV^{-1}
Neutrino ordering	Normal

Lepton unification: the ninths lattice extends naturally to the lepton sector with the same ϵ and the same $1/9$ granularity. Integer-charge models require a separate tuning of the lepton charges and often a different expansion parameter.

IX. SUMMARY AND DISCUSSION

A single discrete \mathbb{Z}_{18} gauge symmetry, whose \mathbb{Z}_9 subgroup governs the flavor sector, simultaneously (i) quantizes flavor hierarchies in ninths, (ii) generates rational Yukawa textures, (iii) protects axion quality via Eq. (15), (iv) fixes E/N and therefore $g_{a\gamma\gamma}$, (v) enforces $N_{\text{DW}} = 1$, and (vi) predicts axion dark matter near $m_a \sim \mathcal{O}(10)$ μeV . Flavor structure and the strong CP solution thus arise from the same discrete gauge origin.

The key numerical results are collected in Table III.

This work sits within a broader program: Paper I [16] established the B -lattice and fit quark and lepton masses; Paper II [17] derived the two-over-two texture from a single flavon with three messenger chains; Paper III [18] parameterized CKM mixing in four magnitudes; Paper IV [19] extended the lattice to the PMNS sector; Paper V [30] provided the dynamical UV completion via vectorlike fermion chains. The present paper (Paper VI) closes the loop by showing that the same discrete symmetry that governs all these flavor structures also solves the strong CP problem, fixes the axion phenomenology, and points to a specific dark-matter mass window.

ACKNOWLEDGMENTS

VB gratefully acknowledges support from the William F. Vilas Estate.

Appendix A: Anomaly Verification

The discrete anomaly conditions of Eq. (14) require that for each SM gauge factor G , the anomaly coefficient $A_G = \sum_i X_i \ell(r_i)$ vanishes mod 18, where X_i is the \mathbb{Z}_{18} charge and $\ell(r_i)$ the Dynkin index ($\ell = 1/2$ for fundamentals).

Using Yukawa invariance, the SM contribution to $A_{SU(3)}$ can be expressed entirely in terms of Higgs and left-handed charges:

$$A_3^{\text{SM}} = \frac{1}{2} \sum_{i=1}^3 [X(Q_i) + X(u_i^c) + X(d_i^c)] \quad (\text{A1})$$

$$= -\frac{3}{2} [X(H_u) + X(H_d)],$$

which is generically nonzero mod 18. The four new vectorlike messenger pairs ($D_a + \bar{D}_a$, $a = 1, \dots, 4$), each a $\mathbf{3} + \bar{\mathbf{3}}$, contribute additional terms:

$$A_3^{\text{VLQ}} = \frac{1}{2} \sum_{a=1}^4 [X(D_a) + X(\bar{D}_a)]. \quad (\text{A2})$$

The \mathbb{Z}_{18} charges of the messenger pairs are chosen so that $A_3^{\text{SM}} + A_3^{\text{VLQ}} \equiv 0 \pmod{18}$. The analogous conditions for $SU(2)_L$ (involving the doublets Q_i , L_i , and any $SU(2)$ components of the messenger sector) and for the mixed \mathbb{Z}_{18} -gravity anomaly ($A_{\text{grav}} = \sum_i X_i$) are similarly satisfied.

The anomaly cancellation thus requires the messenger sector, which is a standard feature of any gauged discrete symmetry construction [11, 12]. The explicit \mathbb{Z}_{18} charge assignments for the full field content (SM fields, Higgs doublets, chain messengers, and flavon) and the numerical verification of all anomaly conditions are given in the companion unified flavor paper [30].

Appendix B: E/N Derivation

We derive $E/N = 8/3$ for the non-supersymmetric case. Using the Yukawa invariance conditions to eliminate right-handed charges:

$$X(u_i^c) = -X(Q_i) - X(H_u), \quad X(d_i^c) = -X(Q_i) - X(H_d), \quad (\text{B1})$$

the QCD anomaly coefficient becomes

$$N = \sum_{i=1}^3 [X(Q_i) + X(u_i^c) + X(d_i^c)] = -3[X(H_u) + X(H_d)]. \quad (\text{B2})$$

Similarly, the electromagnetic anomaly reduces to

$$E = \sum_i X_i Q_i^2 \quad (\text{B3})$$

$$= N_g \left[\frac{2}{3} X(H_u) + \frac{1}{3} X(H_d) \right] + E_\ell,$$

where $E_\ell = \sum_{i=1}^3 [-X(L_i) - X(H_d)] \cdot 1^2 + X(L_i) \cdot 0$ reduces (using lepton Yukawa invariance) to $E_\ell = -3X(H_d)$. Combining:

$$\begin{aligned} \frac{E}{N} &= \frac{3[\frac{2}{3}X(H_u) + \frac{1}{3}X(H_d)] - 3X(H_d)}{-3[X(H_u) + X(H_d)]} \\ &= \frac{2X(H_u) - 2X(H_d)}{-3[X(H_u) + X(H_d)]}. \end{aligned} \quad (\text{B4})$$

For a type-II two-Higgs-doublet model (DFSZ-II) with $X(H_u) = X(H_d) \equiv X_H$, the numerator vanishes at leading order and one must retain the full expression including the lepton contribution. The explicit evaluation, using $E_\ell = -3X(H_d)$ from lepton Yukawa invariance, gives $E/N = 8/3$. This is a standard DFSZ-II result [5] that depends only on the equal-charge Higgs structure, not on the specific values of the matter-field charges.

In the supersymmetric case, the higgsinos \tilde{H}_u and \tilde{H}_d contribute additional terms to both E and N . Their effect shifts E/N from $8/3$ to 2. When the higgsino mass $\mu \gg f_a$, these contributions decouple and E/N reverts to $8/3$.

Appendix C: Messenger Chain Construction

The chain consists of $N_{\text{site}} = 4$ new vectorlike messenger pairs $D_a + \bar{D}_a$ ($a = 1, 2, 3, 4$), all transforming under $SU(3)_C \times SU(2)_L \times U(1)_Y$ as

$$D_a \sim (\mathbf{3}, \mathbf{1}, -1/3), \quad \bar{D}_a \sim (\bar{\mathbf{3}}, \mathbf{1}, +1/3), \quad (\text{C1})$$

i.e. they carry the quantum numbers of right-handed down quarks. Their \mathbb{Z}_9 site charges are $q_9(D_1, D_2, D_3, D_4) = (0, 8, 6, 2)$; the $N_{\text{hop}} = 3$ links connecting adjacent sites carry hop charges $(1, 2, 4)$, which are the differences between neighboring site charges (since $0 - 8 \equiv 1, 8 - 6 = 2, 6 - 2 = 4 \pmod{9}$). The \mathbb{Z}_{18} charges are assigned to satisfy anomaly cancellation (Appendix A).

The SM quarks couple externally to the chain endpoints via

$$\mathcal{L}_{\text{end}} = \lambda_i \bar{q}_{L,i} \tilde{H} D_4 \left(\frac{\Phi}{\Lambda}\right)^{A_i} + \eta_j \bar{D}_1 d_{R,j} \left(\frac{\Phi}{\Lambda}\right)^{B_j} + \text{h.c.}, \quad (\text{C2})$$

where $\tilde{H} = i\sigma_2 H^*$, and the exponents A_i, B_j are fixed by the \mathbb{Z}_{18} charges of the SM fields. The chain Lagrangian itself takes the form

$$\mathcal{L}_{\text{chain}} = \sum_{a=1}^4 M_a \bar{D}_a D_a + \sum_{a=1}^3 \lambda_a \Phi \bar{D}_a D_{a+1} + \text{h.c.}, \quad (\text{C3})$$

where the first sum provides the VLQ mass terms and the second the nearest-neighbor flavon couplings connecting site a to site $a + 1$. When $M_a \sim \Lambda \gg \langle \Phi \rangle$, integrating out all four VLQ pairs generates effective operators with FN suppression ($\langle \Phi \rangle / M_a$) n_a for each traversal of the link between sites a and $a + 1$.

The general chain-inversion theorem [30] shows that the resulting effective Yukawa coupling between SM fields $q_{L,i}$ and $d_{R,j}$ is

$$(Y_d)_{ij} = \lambda_i \eta_j \frac{\prod_{k=1}^3 \kappa_k \epsilon^{h_k/9}}{\prod_{a=1}^4 M_a}, \quad (\text{C4})$$

where κ_k are the $\mathcal{O}(1)$ nearest-neighbor couplings, h_k are the hop charges, and $\epsilon^{(A_i+B_j)/9}$ from the endpoint dressings is absorbed into λ_i and η_j . The rational exponent $p_{ij} = (A_i + \sum_k h_k + B_j)/9$ is thus determined by the endpoint charges plus the hop charges, yielding the ninths-quantized entries of the texture matrices in Eqs. (6)–(9).

For extensions to the up-quark sector and the lepton sector, the messenger content is enlarged to include $SU(2)_L$ doublet messengers. The full construction is developed in Ref. [30].

Appendix D: Terminology: Hops, Sites, and Chains

Because the B -lattice program has developed across several papers, it is useful to collect the key structural distinctions in one place to avoid possible confusion.

Three hop types ($N_{\text{hop}} = 3$): the nearest-neighbor flavon couplings that connect adjacent chain sites. Their \mathbb{Z}_9 charges are $(1, 2, 4)$, equal to the charge differences between neighboring sites. These are the “three messenger chains” referred to in the companion paper [17], which works at the effective-operator level and does not specify the number of VLQ sites.

Four chain sites ($N_{\text{site}} = 4$): the vectorlike quark pairs $D_a + \bar{D}_a$ ($a = 1, 2, 3, 4$) with \mathbb{Z}_9 site charges $(0, 8, 6, 2)$. All four are new heavy fields; the SM quarks couple externally to the endpoints D_1 and D_4 (Appendix C). This is the UV completion developed in the companion unified flavor paper [30].

Backward compatibility: the effective-operator results of the companion papers—the exponent matrices, CKM and PMNS predictions, mass ratio scalings, and $\mathcal{O}(1)$ coefficient fits—depend only on the three hop charges $(1, 2, 4)$ and the endpoint dressings. They are independent of whether the UV completion has three or four VLQ pairs. The distinction matters only for quantities sensitive to the total number of new colored states:

- *Gauge coupling running*: four $\mathbf{3} + \bar{\mathbf{3}}$ pairs shift the one-loop $SU(3)_C$ beta function by $\Delta b_3 = +8/3$. QCD remains asymptotically free ($b_3^{\text{SM}} + \Delta b_3 = -7 + 8/3 = -13/3 < 0$).
- *Discrete anomaly cancellation*: the \mathbb{Z}_{18} anomaly sums receive contributions from all four VLQ pairs (Appendix A).
- *Collider phenomenology*: four species of down-type VLQ are pair-produced at the LHC, each decaying as $D_a \rightarrow bZ, bH, tW$.

Appendix E: Worked Examples: Masses and Mixings from the Chain

We illustrate how quark mass ratios and CKM elements emerge from the exponent matrices in Eq. (6) and the hop framework of Appendix C. Throughout, $\epsilon = 14/75 \approx 0.187$.

1. Calculation rule

Every Yukawa suppression in the ninths framework is obtained by a single rule:

Suppression Rule. For any fermion bilinear $\bar{\psi}_i \psi_j^c H$, the effective Yukawa coupling is

$$Y_{ij} = c_{ij} \epsilon^{p_{ij}}, \quad p_{ij} = Q(\psi_i) + Q(\psi_j^c), \quad (\text{E1})$$

where $Q(\psi_i)$ and $Q(\psi_j^c)$ are the FN charges in Table II, $\epsilon = 14/75$, and c_{ij} is an $\mathcal{O}(1)$ complex coefficient. Mass ratios and mixing angles are then determined by *differences* of exponents:

$$\frac{m_i}{m_j} \sim \epsilon^{p_{ii} - p_{jj}}, \quad \theta_{ij} \sim \epsilon^{|Q(\psi_i) - Q(\psi_j)|}. \quad (\text{E2})$$

For CKM elements, the physical exponents receive an $\mathcal{O}(1/9)$ shift from Fritzsche–Xing phase interference [18].

Table IV collects the resulting suppressions for all diagonal mass ratios and CKM elements.

2. Hops rule

The Suppression Rule gives the exponent p_{ij} from the FN charges. To connect this to the chain diagram in Fig. 2, each charge must be decomposed into flavon insertions at the chain endpoints. Since the flavon carries unit \mathbb{Z}_9 charge, each insertion contributes $1/9$ to the exponent and falls into one of three hop types with charges $(1, 2, 4) \bmod 9$:

TABLE IV. Suppression factors from the calculation rule. Each mass ratio or mixing element is controlled by an exponent p constructed from the FN charges in Table II. The column ϵ^p gives the ninths-framework prediction; “Data” lists the measured value. CKM exponents include the Fritzsche–Xing phase correction.

Observable	Charge rule	p	ϵ^p	Data
<i>Down-type quarks</i>				
m_b	$Q(Q_3) + Q(d_3^c)$	0	1	—
m_s/m_b	$Q(Q_2) + Q(d_2^c)$	7/3	0.020	0.019
m_d/m_b	$Q(Q_1) + Q(d_1^c)$	37/9	0.0010	0.0010
<i>Up-type quarks</i>				
m_t	$Q(Q_3) + Q(u_3^c)$	0	1	—
m_c/m_t	$Q(Q_2) + Q(u_2^c)$	10/3	0.0037	0.0036
m_u/m_t	$Q(Q_1) + Q(u_1^c)$	64/9	6.6×10^{-6}	7.5×10^{-6}
<i>Charged leptons</i>				
m_τ	$Q(L_3) + Q(e_3^c)$	0	1	—
m_μ/m_τ	$Q(L_2) + Q(e_2^c)$	5/3	0.061	0.060
m_e/m_τ	$Q(L_1) + Q(e_1^c)$	29/6	3.0×10^{-4}	2.8×10^{-4}
<i>CKM elements (FX-corrected)</i>				
$ V_{us} $	$\text{FX}(\theta_{12}^d, \theta_{12}^u)$	8/9	0.225	0.225
$ V_{cb} $	$\text{FX}(\theta_{23}^d, \theta_{23}^u)$	17/9	0.042	0.042
$ V_{ub} $	$\text{FX}(\theta_{13}^d, \theta_{13}^u)$	10/3	0.0037	0.0038
$J \sin^{-1} \delta$	$ V_{us} \cdot V_{cb} \cdot V_{ub} $	55/9	3.5×10^{-5}	3.1×10^{-5}

Hops Rule. To compute the suppression for entry (i, j) from the chain diagram (Fig. 2):

1. Look up the charges $Q(\psi_i)$ and $Q(\psi_j^c)$ from Table II.
2. Express $9Q$ as a non-negative integer: $A_i = 9Q(\psi_i)$ (entrance), $B_j = 9Q(\psi_j^c)$ (exit).
3. Decompose each into flavon insertions: $N = n_1 \cdot 1 + n_2 \cdot 2 + n_3 \cdot 4$, where $n_a \geq 0$ counts the number of type- a hops at that endpoint.
4. The full Yukawa suppression is the product of three factors:

$$Y_{ij} \sim \underbrace{\epsilon^{A_i/9}}_{\text{entrance}} \times \underbrace{\epsilon^{7/9}}_{\text{internal}} \times \underbrace{\epsilon^{B_j/9}}_{\text{exit}} = \epsilon^{(A_i + 7 + B_j)/9}. \quad (\text{E3})$$

The internal factor $\epsilon^{7/9} \simeq 0.27$ is common to all entries and sets the overall Yukawa scale (absorbed into m_b, m_t, m_τ). Mass ratios depend only on the endpoint dressings: $m_i/m_j \sim \epsilon^{(A_i + B_i - A_j - B_j)/9}$.

Table V shows the hop decompositions for the diagonal mass-ratio exponents. The third-generation entries require no endpoint flavon insertions ($N = 0$); the first-generation entries require the most, reflecting the depth of the mass hierarchy.

TABLE V. Hop decompositions and endpoint suppressions for the diagonal exponents of Table IV. Here $A_i = 9Q(\psi_i)$ and $B_j = 9Q(\psi_j^c)$ are the ninths numerators of the entrance (left-handed, q_L - D_4 arrow in Fig. 2) and exit (right-handed, D_1 - f_R arrow) endpoint dressings defined in Eq. (C2). The internal chain suppression $\epsilon^{7/9} \simeq 0.27$ is common to all entries and sets the overall Yukawa scale; the total suppression read off from the chain diagram is $\epsilon^{A_i/9} \times \epsilon^{7/9} \times \epsilon^{B_j/9} = \epsilon^{(A_i+7+B_j)/9}$. Since the internal factor cancels in mass ratios, the ratio column ϵ^p lists $\epsilon^{(A_i+B_j)/9}$. The columns (n_1, n_2, n_3) count the type-(1, 2, 4) flavon insertions summed over both endpoints.

Observable	p	A_i	B_j	$\epsilon^{A_i/9}$	$\epsilon^{7/9}$	$\epsilon^{B_j/9}$	Total	ϵ^p	(n_1, n_2, n_3)	n_{tot}
<i>Down-type quarks</i>										
m_b	0	0	0	1	0.27	1	0.27	1	(0, 0, 0)	0
m_s/m_b	7/3	18	3	0.035	0.27	0.57	5.4×10^{-3}	0.020	(1, 0, 5)	6
m_d/m_b	37/9	27	10	0.0065	0.27	0.15	2.7×10^{-4}	0.0010	(1, 0, 9)	10
<i>Up-type quarks</i>										
m_t	0	0	0	1	0.27	1	0.27	1	(0, 0, 0)	0
m_c/m_t	10/3	18	12	0.035	0.27	0.11	1.0×10^{-3}	0.0037	(0, 1, 7)	8
m_u/m_t	64/9	27	37	0.0065	0.27	0.0010	1.8×10^{-6}	6.6×10^{-6}	(0, 0, 16)	16
<i>Charged leptons</i>										
m_τ	0	0	0	1	0.27	1	0.27	1	(0, 0, 0)	0
m_μ/m_τ	5/3	$\frac{9}{2}$	$\frac{21}{2}$	0.43	0.27	0.14	0.016	0.061	—	—
m_e/m_τ	29/6	9	$\frac{69}{2}$	0.19	0.27	0.0016	8.2×10^{-5}	3.0×10^{-4}	—	—

The ‘‘Total’’ column is the full Yukawa suppression $\epsilon^{(A_i+7+B_j)/9}$ as read off from the chain diagram in Fig. 2; the ‘‘ ϵ^p ’’ column divides out the common internal factor $\epsilon^{7/9} \simeq 0.27$ to give the mass ratio relative to the third generation. For quarks, A_i and B_j are integers, so integer hop decompositions always exist. The entrance suppression $\epsilon^{A_i/9}$ is the same for up and down quarks of the same generation (since both share $Q(Q_i)$), while the exit suppressions $\epsilon^{B_j/9}$ differ between the two sectors. For charged leptons, the charges lie on the 1/6 sublattice, so both A_i and B_j can be half-integers; the hop decomposition into integer flavon insertions then requires the full \mathbb{Z}_{18} chain structure of the lepton sector [19], where the relevant integer is $18p$ rather than $9p$ ($18p = 18 \times 5/3 = 30$ for m_μ/m_τ , $18p = 18 \times 29/6 = 87$ for m_e/m_τ).

3. Bottom quark: the unsuppressed entry

The (3, 3) entry of the down-type texture has $p_{33}^d = 0$, since both the third-generation left-handed charge $Q(Q_3) = 0$ and the third-generation right-handed charge $Q(d_3^c) = 0$ vanish. In the chain language, the endpoint couplings $\bar{q}_{L,3} \tilde{H} D_4$ and $\bar{D}_1 d_{R,3}$ carry no additional flavon suppression beyond the chain traversal, and the overall exponent is normalized to zero. The bottom Yukawa coupling is therefore $\mathcal{O}(1)$, setting the reference scale for all other down-type masses.

4. Strange-to-bottom mass ratio

The second-generation diagonal entry is $p_{22}^d = 21/9 = 7/3$, decomposing via the additive rule as

$$p_{22}^d = Q(Q_2) + Q(d_2^c) = \frac{18}{9} + \frac{3}{9} = \frac{21}{9}. \quad (\text{E4})$$

The left-handed contribution $Q(Q_2) = 18/9$ reflects the \mathbb{Z}_9 charge difference between $q_{L,2}$ and $q_{L,3}$: the second-generation doublet requires 18 additional units (in ninths) of flavon suppression at the D_4 endpoint. This decomposes minimally into hops as $18 = 2 \cdot 1 + 0 \cdot 2 + 4 \cdot 4$, i.e. two type-1 hops and four type-4 hops ($n_{\text{tot}} = 6$). The right-handed contribution $Q(d_2^c) = 3/9$ decomposes as $3 = 1 \cdot 1 + 1 \cdot 2 + 0 \cdot 4$ ($n_{\text{tot}} = 2$). The mass ratio prediction is

$$\frac{m_s}{m_b} \sim \epsilon^{7/3} = 0.020, \quad \text{data: } 0.019. \quad (\text{E5})$$

5. Charm-to-top mass ratio

Similarly, $p_{22}^u = 30/9 = 10/3$, with $Q(Q_2) = 18/9$ and $Q(u_2^c) = 12/9 = 4/3$. The right-handed contribution $12 = 0 \cdot 1 + 0 \cdot 2 + 3 \cdot 4$ corresponds to three type-4 hops ($n_{\text{tot}} = 3$). The prediction is

$$\frac{m_c}{m_t} \sim \epsilon^{10/3} = 0.0037, \quad \text{data: } 0.0036. \quad (\text{E6})$$

6. The Cabibbo angle $|V_{us}|$

CKM elements arise from the mismatch between up- and down-type diagonalization rotations. The 1-2 mixing angle in the down sector scales as the ratio of off-diagonal to diagonal entries:

$$\theta_{12}^d \sim \epsilon^{p_{12}^d - p_{22}^d} = \epsilon^{(30-21)/9} = \epsilon, \quad (\text{E7})$$

reflecting the left-handed charge difference $Q(Q_1) - Q(Q_2) = 3 - 2 = 1$ between the first and second generations (the right-handed charges cancel in the ratio). In the up sector, the same left-handed charges give $\theta_{12}^u \sim \epsilon^{(39-30)/9} = \epsilon$. Both 1-2 rotation angles scale as ϵ , but the CKM element $|V_{us}|$ depends on their relative phase. In the Fritzsch–Xing parameterization [18], the phase-dependent interference shifts the effective scaling to

$$|V_{us}| \sim \epsilon^{8/9} = 0.225, \quad \text{data: } 0.225. \quad (\text{E8})$$

The exponent 8/9 is 1/9 less than unity, a direct consequence of the constructive interference between the two $\mathcal{O}(\epsilon)$ rotations at $\phi_{\text{FX}} \approx \pi/2$.

7. The CKM element $|V_{cb}|$

The 2-3 mixing angles in both sectors are controlled by the same left-handed charge difference $Q(Q_2) - Q(Q_3) = 2 - 0 = 2$, giving $\theta_{23}^d \sim \theta_{23}^u \sim \epsilon^{18/9} = \epsilon^2$. Because the leading terms are equal, $|V_{cb}|$ is sensitive to interference and $\mathcal{O}(1)$ coefficients. The effective scaling is

$$|V_{cb}| \sim \epsilon^{17/9} = 0.042, \quad \text{data: } 0.042. \quad (\text{E9})$$

The exponent 17/9 is 1/9 less than 2, again reflecting constructive FX-phase interference.

8. $|V_{ub}|$ and the Jarlskog invariant

The 1-3 CKM element involves the full left-handed charge difference $Q(Q_1) - Q(Q_3) = 3$, but it also factorizes through the FX parameterization as a product of the 1-2 and 2-3 rotations. The effective scaling is

$$|V_{ub}| \sim \epsilon^{10/3} = 0.0037, \quad \text{data: } 0.0038. \quad (\text{E10})$$

The Jarlskog invariant then scales as the product of all three CKM exponents:

$$J \sim \epsilon^{8/9+17/9+10/3} \sin \delta = \epsilon^{55/9} \sin \delta \approx 3.5 \times 10^{-5} \sin \delta, \quad (\text{E11})$$

giving $J \approx 3.1 \times 10^{-5}$ for $\sin \delta \approx 0.88$, consistent with the measured value $(3.08 \pm 0.13) \times 10^{-5}$.

9. Muon-to-tau mass ratio

As a lepton-sector example, the muon-to-tau mass ratio is controlled by the lepton-doublet and right-handed charge differences between the second and third generations: $Q(L_2) - Q(L_3) = 1/2$ and $Q(e_2^c) - Q(e_3^c) = 7/6$. The diagonal entry $p_{22}^\ell = Q(L_2) + Q(e_2^c) = 1/2 + 7/6 = 5/3$ directly gives the mass ratio:

$$\frac{m_\mu}{m_\tau} \sim \epsilon^{5/3} = 0.061, \quad \text{data: } 0.060. \quad (\text{E12})$$

Note that the lepton charges lie on the 1/6 sublattice of the 1/18 lattice (since $18 \times 1/6 = 3$ and $18 \times 7/6 = 21$ are integers), reflecting the bilinear structure of the charged-lepton Yukawa operator. The lepton sector uses the same expansion parameter $\epsilon = 14/75$ as the quark sector, illustrating the quark-lepton universality of the ninths framework.

-
- [1] R. D. Peccei and H. R. Quinn, “CP conservation in the presence of pseudoparticles,” *Phys. Rev. Lett.* **38**, 1440 (1977).
- [2] S. Weinberg, “A new light boson?,” *Phys. Rev. Lett.* **40**, 223 (1978).
- [3] F. Wilczek, “Problem of strong P and T invariance in the presence of instantons,” *Phys. Rev. Lett.* **40**, 279 (1978).
- [4] J. E. Kim and G. Carosi, “Axions and the strong CP problem,” *Rev. Mod. Phys.* **82**, 557 (2010), arXiv:0807.3125.
- [5] L. Di Luzio, M. Giannotti, E. Nardi, and L. Visinelli, “The landscape of QCD axion models,” *Phys. Rep.* **870**, 1 (2020), arXiv:2003.01100.
- [6] M. Kamionkowski and J. March-Russell, “Planck scale physics and the Peccei-Quinn mechanism,” *Phys. Lett. B* **282**, 137 (1992), arXiv:hep-th/9202003.
- [7] R. Holman, S. D. H. Hsu, T. W. Kephart, E. W. Kolb, R. Watkins, and L. M. Widrow, “Solutions to the strong CP problem in a world with gravity,” *Phys. Lett. B* **282**, 132 (1992), arXiv:hep-ph/9203206.
- [8] S. M. Barr and D. Seckel, “Planck scale corrections to axion models,” *Phys. Rev. D* **46**, 539 (1992).
- [9] L. M. Krauss and F. Wilczek, “Discrete gauge symmetry in continuum theories,” *Phys. Rev. Lett.* **62**, 1221 (1989).
- [10] K. S. Babu, I. Gogoladze, and K. Wang, “Stabilizing the axion by discrete gauge symmetries,” *Phys. Lett. B* **560**, 214 (2003), arXiv:hep-ph/0212339.
- [11] L. E. Ibáñez and G. G. Ross, “Discrete gauge symmetries and the origin of baryon and lepton number conservation in supersymmetric versions of the standard model,” *Phys. Lett. B* **260**, 256 (1991).
- [12] T. Banks and M. Dine, “Note on discrete gauge anomalies,” *Phys. Rev. D* **45**, 1424 (1992), arXiv:hep-

- th/9109045.
- [13] C. D. Froggatt and H. B. Nielsen, “Hierarchy of quark masses, Cabibbo angles and CP violation,” *Nucl. Phys. B* **147**, 277 (1979).
- [14] M. Leurer, Y. Nir, and N. Seiberg, “Mass matrix models,” *Nucl. Phys. B* **398**, 319 (1993), arXiv:hep-ph/9212278.
- [15] M. Leurer, Y. Nir, and N. Seiberg, “Mass matrix models: The sequel,” *Nucl. Phys. B* **420**, 468 (1994), arXiv:hep-ph/9310320.
- [16] V. Barger, “One-flavon flavor: A single hierarchical parameter B organizes quarks and leptons at M_Z ,” *Phys. Rev. D* **113**, 013002 (2026), arXiv:2512.13630.
- [17] V. Barger, “Two-over-Two Lattice Flavor from a Single Flavon with Three Messenger Chains,” *Phys. Rev. D* (in press), arXiv:2602.18393.
- [18] V. Barger, “Quark Mixing from a Lattice Flavon Model: A Four-Magnitude Parameterization,” submitted to *Phys. Rev. D*, arXiv:2603.00810.
- [19] V. Barger, “Lepton Masses and Mixing from the B -Lattice Flavon Framework,” submitted to *Phys. Rev. D* (2026).
- [20] P. Sikivie, “Of axions, domain walls and the early universe,” *Phys. Rev. Lett.* **48**, 1156 (1982).
- [21] K. S. Babu, S. C. Chandrasekar, and Z. Tavartkiladze, “Peccei–Quinn symmetry from a gauged flavor symmetry,” arXiv:2602.24253.
- [22] C. Cornella, D. Curtin, G. Neil, and L. Thompson, “Mapping the Froggatt–Nielsen landscape of quark flavor,” *Phys. Rev. D* **111**, 075015 (2025), arXiv:2306.08026.
- [23] C. Cornella, D. Curtin, G. Neil, and L. Thompson, “Froggatt–Nielsen models with a residual \mathbb{Z}_2 ,” arXiv:2501.00629.
- [24] N. Cabibbo, “Unitary symmetry and leptonic decays,” *Phys. Rev. Lett.* **10**, 531 (1963).
- [25] M. Kobayashi and T. Maskawa, “CP-violation in the renormalizable theory of weak interaction,” *Prog. Theor. Phys.* **49**, 652 (1973).
- [26] S. Navas *et al.* (Particle Data Group), “Review of particle physics,” *Phys. Rev. D* **110**, 030001 (2024).
- [27] C. Jarlskog, “Commutator of the quark mass matrices in the standard electroweak model and a measure of maximal CP nonconservation,” *Phys. Rev. Lett.* **55**, 1039 (1985).
- [28] G.-Y. Huang and S. Zhou, “Precise values of running quark and lepton masses in the standard model,” *Phys. Rev. D* **103**, 016010 (2021), arXiv:2009.04851.
- [29] S. Weinberg, “Baryon- and lepton-nonconserving processes,” *Phys. Rev. Lett.* **43**, 1566 (1979).
- [30] V. Barger, “Unified Flavor Program: Lattice Quantization, Chain Locality, and a Dynamical Origin of Hierarchical Yukawas,” submitted to *Phys. Rev. D* (2026).
- [31] J. E. Kim, “Weak-interaction singlet and strong CP invariance,” *Phys. Rev. Lett.* **43**, 103 (1979).
- [32] M. A. Shifman, A. I. Vainshtein, and V. I. Zakharov, “Can confinement ensure natural CP invariance of strong interactions?,” *Nucl. Phys. B* **166**, 493 (1980).
- [33] M. Dine, W. Fischler, and M. Srednicki, “A simple solution to the strong CP problem with a harmless axion,” *Phys. Lett. B* **104**, 199 (1981); A. R. Zhitnitsky, *Sov. J. Nucl. Phys.* **31**, 260 (1980).
- [34] P. N. Bhattiprolu and S. P. Martin, “Discrete gauge symmetries from (broken) continuous gauge symmetries,” *Phys. Rev. D* **104**, 055014 (2021), arXiv:2106.14964.
- [35] H. Baer, V. Barger, and D. Sengupta, “Axion quality problem with Pati–Salam,” *Phys. Lett. B* **790**, 58 (2019), arXiv:1810.03713.
- [36] K. J. Bae, H. Baer, and H. Serce, “Prospects for axion detection in natural SUSY with mixed axion-higgsino dark matter: back to invisible?,” *J. Cosmol. Astropart. Phys.* **06**, 024 (2017), arXiv:1705.01134.
- [37] C. Bartram *et al.* (ADMX Collaboration), “Search for Axion Dark Matter from 1.1 to 1.3 GHz with ADMX,” arXiv:2504.07279.
- [38] S. Navas *et al.* (Particle Data Group), *Phys. Rev. D* **110**, 030001 (2024), see also the “Axions and Other Similar Particles” review at pdg.lbl.gov.
- [39] D. J. E. Marsh, “Axion cosmology,” *Phys. Rep.* **643**, 1 (2016), arXiv:1510.07633.
- [40] V. B. Klaer and G. D. Moore, “The dark-matter axion mass,” *J. Cosmol. Astropart. Phys.* **11**, 049 (2017), arXiv:1708.07521.
- [41] M. Buschmann, R. T. Co, C. Dessert, and B. R. Safdi, “Axion emission can explain a new hard x-ray excess from nearby isolated neutron stars,” *Phys. Rev. Lett.* **129**, 161301 (2022), arXiv:2108.05368.
- [42] M. Gorghetto, E. Hardy, and G. Villadoro, “More axions from strings,” *SciPost Phys.* **10**, 050 (2021), arXiv:2007.04990.
- [43] Y. Akrami *et al.* (Planck Collaboration), “Planck 2018 results. X. Constraints on inflation,” *Astron. Astrophys.* **641**, A10 (2020), arXiv:1807.06211.
- [44] M. Hindmarsh, J. Davies, and M. Lilley, “Axion string wall collisions and their cosmological consequences,” *Phys. Rev. D* **103**, 103534 (2021), arXiv:2102.07723.
- [45] I. Esteban, M. C. Gonzalez-Garcia, M. Maltoni, I. Martinez-Soler, J. P. Pinheiro, and T. Schwetz, “NuFit-6.0: Updated global analysis of three-flavor neutrino oscillations,” *JHEP* **12**, 216 (2024), arXiv:2410.05380; see also <https://www.nu-fit.org>.
- [46] B. Pontecorvo, “Mesonium and antimesonium,” *Zh. Eksp. Teor. Fiz.* **33**, 549 (1957) [*Sov. Phys. JETP* **6**, 429 (1958)].
- [47] Z. Maki, M. Nakagawa, and S. Sakata, “Remarks on the unified model of elementary particles,” *Prog. Theor. Phys.* **28**, 870 (1962).
- [48] P. F. Harrison and W. G. Scott, “ μ – τ reflection symmetry in lepton mixing and neutrino oscillations,” *Phys. Lett. B* **547**, 219 (2002), arXiv:hep-ph/0210197.
- [49] C. S. Lam, “Symmetry of lepton mixing,” *Phys. Lett. B* **656**, 193 (2007), arXiv:0708.3665.
- [50] B. Abi *et al.* (DUNE Collaboration), “Deep Underground Neutrino Experiment (DUNE), Far Detector Technical Design Report, Volume II: DUNE Physics,” arXiv:2002.03005 (2020).
- [51] K. Abe *et al.* (Hyper-Kamiokande Collaboration), “Hyper-Kamiokande Design Report,” arXiv:1805.04163 (2018).
- [52] J. A. Aguilar-Saavedra, R. Benbrik, S. Heinemeyer, and M. Pérez-Victoria, “Handbook of vectorlike quarks: Mixing and single production,” *Phys. Rev. D* **88**, 094010 (2013), arXiv:1306.0572.